

MICROSTRUCTURE OPTIMISATION OF CENTRIFUGALLY CAST IN-SITU TiAl-BASED MATRIX COMPOSITE REINFORCED WITH Ti₂AlC PARTICLES

Kateryna KAMYSHNYKOVA, Juraj LAPIN

Institute of Materials and Machine Mechanics, Slovak Academy of Sciences, Bratislava, Slovakia, EU
kateryna.kamyshnykova@savba.sk, juraj.lapin@savba.sk

<https://doi.org/10.37904/metal.2019.942>

Abstract

Samples of in-situ TiAl-based matrix composite reinforced with Ti₂AlC particles were prepared by the centrifugal casting of Ti-47Al-5Nb-1C-0.2B (at.%) alloy. The as-cast samples were subjected to hot isostatic pressing (HIP) at 1360 °C to remove casting porosity. The applied HIP conditions resulted in a significant coarsening of as-cast grain structure connected with deterioration of mechanical properties. Two multi-stage heat treatment routes were proposed to refine the coarse grain structure of the HIP-ed samples. The pre-treatment of the composite in single α phase field followed by air cooling (AC), oil quenching (OQ) or water quenching (WQ) leads to the formation of massive γ_M (TiAl). The consequent annealing in the γ (TiAl) phase field followed by a stabilisation annealing at 900 °C leads to the formation of homogeneous fine-grained γ type of microstructure in the OQ and WQ samples. The solution annealing of the OQ and WQ samples in the α phase field followed by slow cooling results in the formation of refined equiaxed grains with nearly lamellar α_2 (Ti₃Al) + γ microstructure. The contribution of several mechanisms to the grain refinement is analysed and discussed.

Keywords: TiAl, composites, casting, heat treatments, microstructure

1. INTRODUCTION

TiAl-based alloys are attractive materials for industrial applications due to their light weight and a good combination of properties [1]. These alloys allow reducing the weight of aircraft engines and improve the dynamic characteristics of turbochargers of combustion engines [2]. However, their inherent poor ductility at room temperature and insufficient strength at high temperatures limit their wide-scale applications. Intermetallic matrix composites may improve the deficiency of these alloys at high temperatures because of the good combination of the properties of the intermetallic TiAl matrix and ceramic reinforcement. Among various ceramics, layered ternary MAX phases (M is a transition metal, A is an A-group element and X is nitrogen or carbon) such as Ti₂AlC shows a significant role in reinforcing and toughening of in-situ TiAl-based matrix composites [3-6].

The most cost-effective route for the production of complex shaped TiAl-based components such as turbocharger wheels, turbine blades or exhaust valves is precision casting [7,8]. Centrifugal precision casting leads to better surface quality, no misruns in thin sections and fewer cracks compared to those of gravity cast components [9]. The centrifugal casting can be combined with different types of melting but the induction melting is the most frequently used technique due to its flexibility. The casting leads usually to the formation of coarse-grained and inhomogeneous microstructures in TiAl-based alloys.

Basically, two main approaches have been investigated to refine the coarse-grained structure of as-cast TiAl-based alloys: (i) solid-state phase transformations and (ii) alloying with minor additions. According to the importance of diffusion, the solid-state phase transformations can be divided into two groups: (i) diffusionless massive transformation and (ii) diffusion-related transformations such as lamellar, Widmanstätten lamellar and feathery. Heat treatments inducing massive γ_M (TiAl) transformation are considered as a possible way to refine the grain size and reduce the texture without modifying the shape of the cast components [10-12].

The aim of this article is to optimise microstructure of centrifugally cast in-situ TiAl-based matrix composite reinforced with Ti₂AlC particles with a nominal composition Ti-47Al-5Nb-1C-0.2B (at.%). In this alloy, niobium is added to improve oxidation resistance and strength properties at both room and high temperatures [13]. Boron refines grain microstructure and carbon improves high temperature strength [14,15].

2. EXPERIMENTAL PROCEDURE

The samples of in-situ composite with a nominal composition Ti-47Al-5Nb-1C-0.2B (at.%) were prepared by centrifugal casting in the form of conical samples with a minimum diameter of 15 mm, maximum diameter of 17 mm and length of 150 mm. The charge was placed into a graphite crucible with a diameter of 49 mm (outside diameter) and length of 75 mm. Each graphite crucible was put into a protective alumina crucible equipped with a pouring cup which was connected to a cylindrical graphite mould. The melt was centrifugally cast into the graphite mould.

Hot isostatic pressing (HIP) was applied to remove casting porosity. The as-cast samples were put into alumina crucible, heated to a temperature of 1360 °C and hold at this temperature under a pressure of 200 MPa for 4 h in argon. The cooling of the HIP-ed samples to room temperature was carried out in the HIP apparatus at an average rate of 8 °C/min.

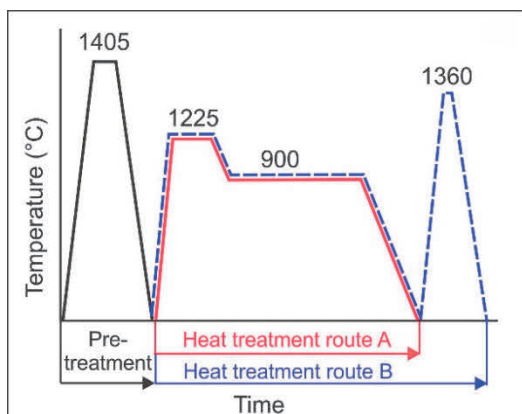


Figure 1 Schematic views of the applied heat treatment routes.

Heat treatment experiments were performed on the HIP-ed samples. The pre-treatment of the samples consisted of solution annealing at a temperature of 1405 °C for 1 h under protective argon atmosphere and cooling in three different mediums: forced air, oil and water. The pre-treated samples were subjected to two types of heat treatment designated as heat treatment route A (red solid curve) and heat treatment route B (blue dashed curve), as schematically shown in **Figure 1**. The heat treatment route A consisted of annealing at a temperature of 1225 °C for 4 h in argon followed by stabilisation annealing at a temperature of 900 °C for 20 h in air. The heat treatment route B included annealing of the pre-treated samples at 1225 °C for 4 h in argon, stabilisation annealing at 900 °C for 20 h in air, cooling to room temperature followed by annealing at

1360 °C for 0.5 h in argon and was finalised by cooling to room temperature at a rate of 10 °C/min.

Metallographic preparation of the samples consisted of a standard grinding using abrasive papers, polishing on diamond pastes and etching in a solution of 100 ml H₂O, 6 ml HNO₃ and 3 ml HF. Microstructure evaluation was performed by optical microscopy (OM), scanning electron microscopy (SEM) and scanning electron microscopy in back-scattered electron (BSE) mode. Volume fraction of phases was measured by computerised image analysis using digitalised micrographs. Grain size was measured by a linear intercept method and the measured data were treated statistically.

3. RESULTS AND DISCUSSION

3.1. Microstructure of as-cast and HIP-ed in-situ composite

Figure 2 shows the typical microstructure of the centrifugally cast samples. The microstructure consists of equiaxed grains with nearly lamellar structure and some small interdendritic porosity. The grains contain plate-like particles distributed preferentially within the dendrites and ribbon-like particles formed in the

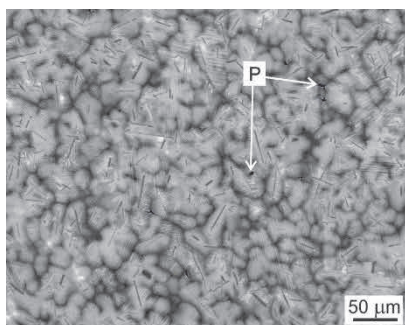


Figure 2 Centrifugally cast in-situ composite, P - porosity, BSE.

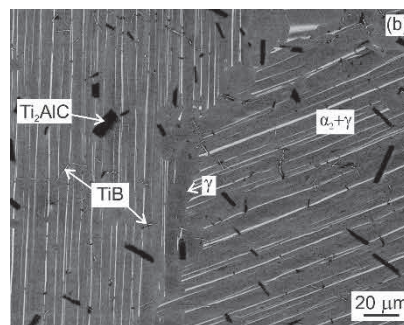
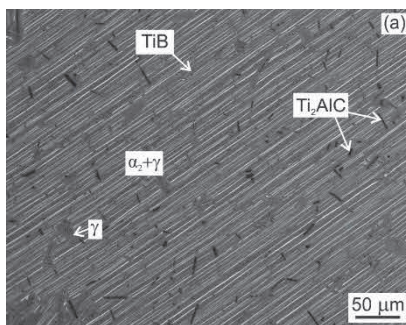


Figure 3 BSE micrographs of the in-situ composite after the HIP: (a) fully lamellar microstructure; (b) serrated grain boundary.

interdendritic region. The XRD analysis has indicated the presence of four phases: γ (TiAl), α_2 (Ti₃Al), Ti₂AlC and TiB [3]. The mean grain size, mean length of plate-like Ti₂AlC particles and volume fraction of carbide particles are measured to be $(53.1 \pm 1.2) \mu\text{m}$, $(15.7 \pm 0.2) \mu\text{m}$ and $(2.3 \pm 0.2) \text{vol.}\%$, respectively.

The closed porosity in the centrifugally cast in-situ composite can be successfully removed by the HIP, as shown in **Figure 3**. However, the applied HIP at a temperature of 1360 °C corresponding to a single α phase field leads to the formation of coarse-grained fully lamellar microstructure with some grains exceeding 1000 μm , as seen in **Figure 3a**. The driving force for the growth of the coarse grains is the plastic deformation and strain energy stored in the deformed regions of the samples due to the collapse of the porosity during HIP [16]. The amount of plastic deformation is a maximum at the surface of shrinkage porosity and decreases with the distance from the porosity. The nucleation and growth of the recrystallized α (Ti-based solid solution with a hexagonal crystal structure) grains occur predominantly at the central region of the HIP-ed samples where the porosity is filled with the deformed material. When the sample is cooled from the HIP temperature, the α grains decompose by the nucleation and growth of γ lath to lamellar $\alpha + \gamma$ type of microstructure. **Figure 3b** shows that the microstructure of the HIP-ed sample is fully lamellar and consists of well-aligned α_2 and γ laths, plate-like Ti₂AlC particles and ribbon-like borides. The serrated grain boundaries contain predominantly the γ phase. Since the coarse-grained microstructure deteriorates room-temperature ductility of TiAl-based alloys [17], additional heat treatments are required to optimise the microstructure of the in-situ composite after the applied HIP.

3.2. Pre-treatment of HIP-ed samples

Figure 4 shows the microstructure of the samples after the pre-treatment consisting of solution annealing in a single α phase field at 1405 °C for 1 h in argon followed by air cooling (AC), oil quenching (OQ) and water quenching (WQ) to room temperature. It is clear from **Figure 4** that the nucleation and growth of massive γ_M depend strongly on the applied cooling medium. The microstructure of the AC sample remains predominantly lamellar with a low volume fraction of the massive γ_M (3 vol.%), as illustrated in **Figure 4a**. The OQ leads to an increase of the volume fraction of the massive γ_M to 17.5 vol.%, the formation of lamellar $\alpha_2 + \gamma$ regions and preservation of retained α_R phase in the microstructure, as seen in **Figure 4b**. Further increase of the volume fraction of the massive γ_M to 30.0 vol.% and preservation of the retained α_R phase is achieved after the WQ, as shown in **Figure 4c**.

Since the coarse-grained microstructure of the HIP-ed samples limits significantly the length of grain boundaries, which represent effective nucleation sites for the massive γ_M , only less effective heterogeneous nucleation of the massive γ_M grains occurs on the defects within the α grains [11]. However, the WQ of the studied in-situ composite results in the relatively low volume fraction of the massive γ_M counterbalanced by stabilisation of the retained α_R phase in the microstructure. The high amount of the α_R can be attributed to its

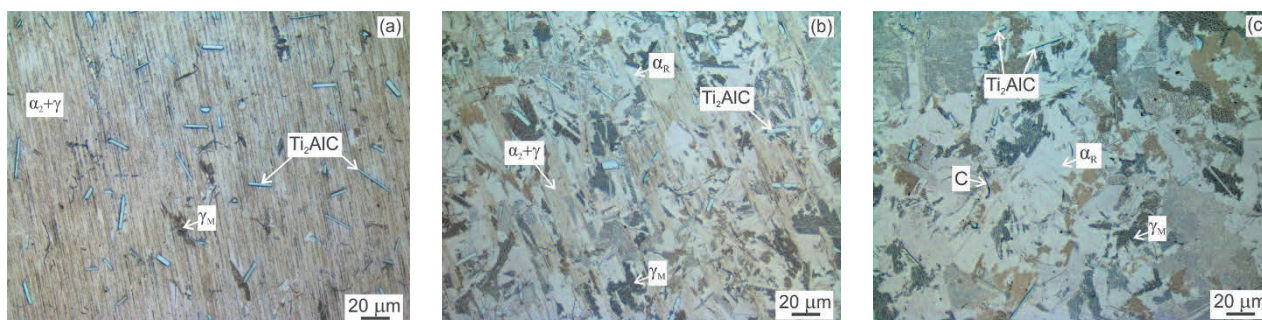


Figure 4 OM micrographs showing the typical microstructures of the samples subjected to the pre-treatment: (a) air cooling (AC); oil quenching (OQ); (c) water quenching (WQ), C - crack.

stabilisation by a relatively high content of carbon. It should be noted, that the massive γ_M grains contain a large number of crystal defects such as dislocations, stacking faults and anti-phase boundaries. The microstructure of the pre-treated in-situ composite containing massive γ_M grains is not stable at high temperatures and need to be stabilised by additional treatments.

3.3. Heat treatment route A

Figure 5 shows the microstructure of the pre-treated AC, OQ and WQ samples subjected to the heat treatment route A. The microstructure of the AC sample consists of coarse grains with partially decomposed lamellar $\alpha_2 + \gamma$ microstructure and local regions with small recrystallized γ grains (10 vol.%), as shown in **Figure 5a**. The statistical analysis of the measured grain size leads to a log-normal distribution function with a mean size of the recrystallized γ grains of $(7.5 \pm 0.2) \mu m$. It should be noted that the large lamellar colonies with an average size of $(335 \pm 23) \mu m$ still remain in the central part of the AC samples. The applied two-step annealing at $1225^\circ C$ and $900^\circ C$ leads to a significant grain refinement of the samples subjected to OQ (**Figure 5b**) and WQ (**Figure 5c**). The mean grain size is measured to be $(6.1 \pm 0.1) \mu m$ and $(5.9 \pm 0.1) \mu m$ for the OQ and WQ samples, respectively. The driving force and kinetic conditions for the formation of small recrystallized γ grains during annealing at a temperature of $1225^\circ C$ corresponding to a single γ phase field are the internal stresses together with the defects induced by the quenching in the α phase. Since the solubility of carbon is significantly lower in the γ (0.3 at.%) than in the α_2 phase (1.2 at.%) [18], the formation of the equiaxed γ type of microstructure is accompanied with intensive precipitation of the carbide particles during the annealing, as seen in **Figures 5b** and **5c**. These fine carbide particles are preferentially distributed along the γ grain boundaries and can act as very effective obstacles hindering grain boundary sliding during high temperature creep.

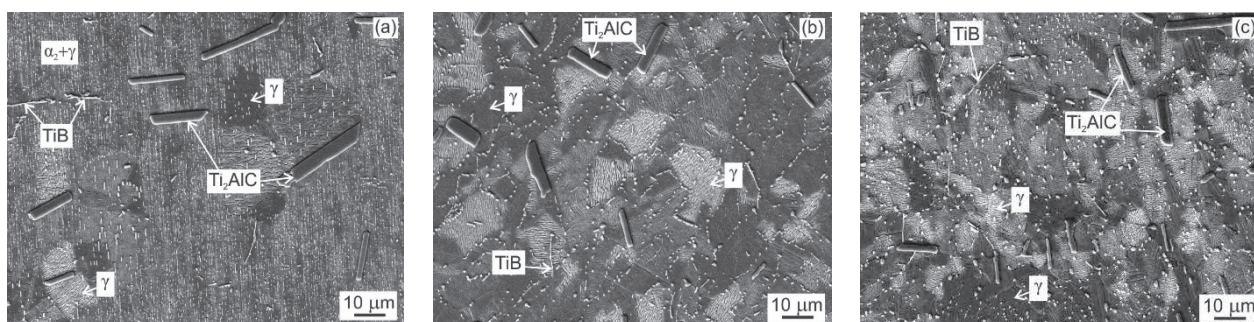


Figure 5 SEM micrographs showing the typical microstructures of the pre-treated samples subjected to the heat treatment route A: (a) AC; (b) OQ; (c) WQ

3.4. Heat treatment route B

Figure 6 shows the microstructure of the pre-treated AC, OQ and WQ samples subjected to the heat treatment route B. The microstructure of the AC samples consists of large lamellar grains, as shown in **Figure 6a**. The mean grain size is measured to be $(389 \pm 15) \mu\text{m}$. The microstructure of the OQ and WQ samples is nearly lamellar and besides well-aligned α_2 and γ lamellae contain coarse irregular shaped α_2 particles randomly distributed in the γ matrix, as seen in **Figures 6b** and **6c**. The mean grain size is measured to be $(77.6 \pm 2.1) \mu\text{m}$ and $(53.9 \pm 1.9) \mu\text{m}$ for the OQ and WQ samples, respectively. A good balance between creep strength and room temperature ductility can be achieved in fine-grained alloys with fully lamellar microstructure. However, fine lamellae are usually unstable and degrade during creep deformation which leads to a decrease in creep strength [19,20].

The achieved results indicate that the microstructure of the studied in-situ composite can be tailored from the coarse-grained fully lamellar $\alpha_2 + \gamma$ to fine-grained γ type by the appropriate heat treatments. It should be noted that the WQ and occasionally OQ could lead to the formation of cracks in the in-situ composite. Hence, such types of cooling cannot be used for processing of reliable defect free complex-shaped components in the production.

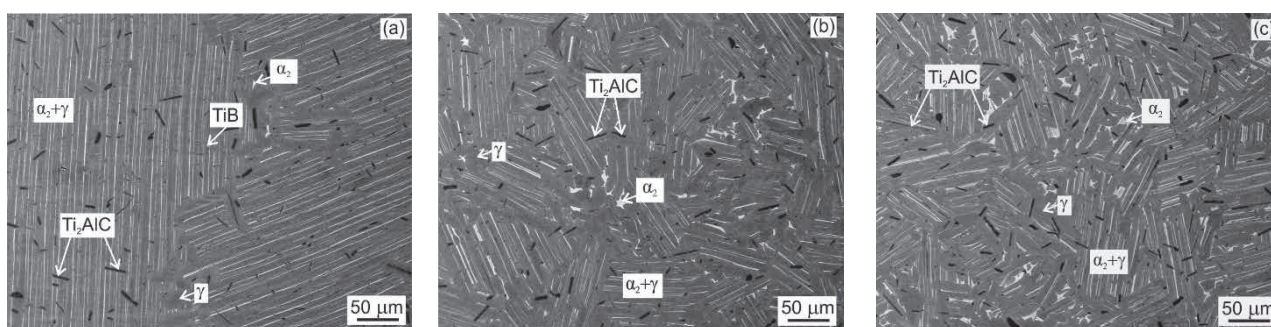


Figure 6 BSE micrographs showing the typical microstructures of the pre-treated samples subjected to the heat treatment route B: (a) AC; (b) OQ; (c) WQ

4. CONCLUSIONS

The microstructure optimisation of centrifugally cast in-situ TiAl-based matrix composite with a nominal composition Ti-47Al-5Nb-1C-0.2B (at.%) reinforced with Ti_2AlC particles was studied with the aim to remove casting porosity, homogenise the as-cast microstructure and control the size of fully lamellar grains. The following conclusions are reached:

- The microstructure of the centrifugally cast in-situ composite consists of equiaxed nearly lamellar $\alpha_2 + \gamma$ grains, plate-like Ti_2AlC particles and ribbon-like TiB borides. The applied HIP in the α phase field removes fully casting porosity but leads to the growth of coarse grains which need to be refined by appropriate heat treatments.
- The pre-treatment of the HIP-ed in-situ composite in α phase field and subsequent AC, OQ and WQ lead to the formation of massive γ_M . The volume fraction of massive γ_M depends on the cooling medium and increases with changing cooling medium from forced air to water.
- The heat treatment route A of the pre-treated in-situ composite leads to the formation of the equiaxed γ grains with partially decomposed α_2 lamellae and numerous fine carbide precipitates, which are formed along the grain boundaries. The heat treatment route B results in the formation of the equiaxed nearly lamellar $\alpha_2 + \gamma$ grains with a mean grain size ranging from 53.9 to 389 μm .

ACKNOWLEDGEMENTS

This work was financially supported by the Slovak Research and Development Agency under the contract APVV-15-0660.

REFERENCES

- [1] SUNG, S.Y. and KIM, Y.J. Alpha-case formation mechanism on titanium investment castings. *Mater. Sci. Eng. A*. 2005. vol. 405, pp. 173-177. DOI:10.1016/J.MSEA.2005.05.092.
- [2] BEWLAY, B.P., NAG, S., SUZUKI, A. and WEIMER, M.J. TiAl alloys in commercial aircraft engines. *Mater. High Temp.* 2016. vol.33, pp. 549-559. DOI:10.1080/09603409.2016.1183068.
- [3] LAPIN, J. and KAMYSHNYKOVA, K. Processing, microstructure and mechanical properties of in-situ Ti₃Al+TiAl matrix composite reinforced with Ti₂AlC particles prepared by centrifugal casting. *Intermetallics*. 2018. vol. 98, pp. 34-44. DOI:10.1016/j.intermet.2018.04.012.
- [4] ŠTAMBORSKÁ, M., LAPIN, J. and BAJANA, O. Effect of carbon on the room temperature compressive behaviour of Ti-44.5Al-8Nb-0.8Mo-x C alloys prepared by vacuum induction melting. *Kov. Mater.* 2018. vol. 56, pp. 349-356. DOI:10.4149/km_2018_6_349.
- [5] ČEGAN, T. and SZURMAN, I. Thermal stability and precipitation strengthening of fully lamellar Ti-45Al-5Nb-0.2B-0.75C alloy. *Kov. Mater.* 2018. vol. 55, pp. 421-430. DOI:10.4149/km_2017_6_421.
- [6] LAPIN, J., ŠTAMBORSKÁ, M., PELACHOVÁ, T. and BAJANA, O. Fracture behaviour of cast in-situ TiAl matrix composite reinforced with carbide particles. *Mater. Sci. Eng. A*. 2018. vol. 721, pp. 1-7. DOI:10.1016/j.msea.2018.02.077.
- [7] TETSUI, T., KOBAYASHI, T., KISHIMOTO, A. and HARADA, H. Structural optimization of an yttria crucible for melting TiAl alloy. *Intermetallics*. 2012. vol. 20, pp.16-23. DOI:10.1016/j.intermet.2011.08.026.
- [8] HARDING, R.A., WICKINS, M., WANG, H., DJAMBAZOV, G. and PERICLEOUS, K.A. Development of a turbulence-free casting technique for titanium aluminides. *Intermetallics*. 2011. vol. 19, pp. 805-813. DOI:10.1016/j.intermet.2010.11.022.
- [9] HARDING, R.A. Recent developments in the induction skull melting and investment casting of titanium aluminides. *Kov. Mater.* 2004. vol. 42, pp. 225-241.
- [10] CLEMENS, H., BARTELS, A., BYSTRZANOWSKI, S., CHLADIL, H., LEITNER, H., DEHM, G., GERLING, R. and SCHIMANSKY, F.P. Grain refinement in γ -TiAl-based alloys by solid state phase transformations. *Intermetallics*. 2006. vol. 14, pp. 1380-1385. DOI:10.1016/j.intermet.2005.11.015.
- [11] SANKARAN, A., BOUZY, E., HUMBERT, M. and HAZOTTE, A. Variant selection during nucleation and growth of γ_m -massive phase in TiAl-based intermetallic alloys. *Acta Mater.* 2009. vol. 57, pp. 1230-1242. DOI:10.1016/j.actamat.2008.11.012.
- [12] KAMYSHNYKOVA, K. and LAPIN, J. Grain refinement of cast peritectic TiAl-based alloy by solid-state phase transformations. *Kov. Mater.* 2018. vol. 56, pp. 277-287. DOI:10.4149/km_2018_5_277.
- [13] LIN, J.P., ZHAO, L.L., LI, G.Y., ZHANG, L.Q., SONG, X.P., YE, F. and CHEN, G.L. Effect of Nb on oxidation behavior of high Nb containing TiAl alloys. *Intermetallics*. 2011. vol.19, pp.131-136. DOI:10.1016/J.INTERMET.2010.08.029.
- [14] HECHT, U., WITUSIEWICZ, V., DREVERMANN, A. and ZOLLINGER, J. Grain refinement by low boron addition in niobium-rich TiAl-based alloys. *Intermetallics*. 2008. vol.16, pp. 969-978. DOI:10.1016/j.intermet.2008.04.019.
- [15] SCHWAIGHOFER, E., RASHKOVA, B., CLEMENS, H., STARK, A. and MAYER, S. Effect of carbon addition on solidification behavior, phase evolution and creep properties of an intermetallic β -stabilized γ -TiAl based alloy. *Intermetallics*. 2014. vol. 46, pp.173-184. DOI:10.1016/j.intermet.2013.11.011.
- [16] JEON, J.H., GODFREY, A.B., BLENKINSOP, P.A., VOICE, W. and HAHN, Y.D. Recrystallization in cast 45-2-2 XDTM titanium aluminide during hot isostatic pressing. *Mater. Sci. Eng. A*. 1999. vol. 271, pp.128-133. DOI:10.1016/S0921-5093(99)00192-6.
- [17] KIM, Y.W. Effects of microstructure on the deformation and fracture of γ -TiAl alloys. *Mater. Sci. Eng. A*. 1995. vol.192-193, pp. 519-533. DOI:10.1016/0921-5093(94)03271-8.

- [18] ZHANG, H., DING, H., WANG, Q., CHEN, R. and GUO, J. Microstructures and tensile properties of directionally solidified Ti-45Al-2Cr-2Nb alloy by electromagnetic cold crucible zone melting technology with Y₂O₃ moulds. *Vacuum*. 2018. vol. 148, pp. 206-213. DOI:10.1016/j.vacuum.2017.11.032.
- [19] WANG, Q., CHEN, R., YANG, Y., WU, S., GUO, J., DING, H., SU, Y. and FU, H. Effects of lamellar spacing on microstructural stability and creep properties in β -solidifying γ -TiAl alloy by directional solidification. *Mater. Sci. Eng. A*. 2018. vol. 711, pp. 508-514. DOI:10.1016/j.msea.2017.11.080.
- [20] HUANG, Z.W., LIN, J.P. and SUN, H.L. Microstructural changes and mechanical behaviour of a near lamellar γ -TiAl alloy during long-term exposure at 700 °C. *Intermetallics*. 2017. vol. 85, pp. 59-68. DOI:10.1016/j.intermet.2017.02.002.